AEC RESEARCH AND
DEVELOPMENT REPORT

HW-69945

THERMAL CONDUCTIVITY OF UO_2

J. L. DANIEL
J. MATOLICH, Jr. and H. W. DEEM

SEPTEMBER, 1962

HANFORD LABORATORIES

HANFORD ATOMIC PRODUCTS OPERATION
RICHLAND, WASHINGTON

GENERAL ELECTRIC

LEGAL NOTICE

AEC-GE RICHLAND, WASH.

HW-69945

UC-25, Metals, Ceramics,
and Materials
(TID-4500, 18th Ed.)

THERMAL CONDUCTIVITY OF UO_2

By

J. L. Daniel

Ceramics Research
Reactor and Fuels Research and Development Operation
Hanford Laboratories

and

J. Matolich, Jr., and H. W. Deem

Instrumentation Division
Battelle Memorial Institute
Columbus, Ohio

September, 1962

HANFORD ATOMIC PRODUCTS OPERATION
RICHLAND, WASHINGTON

Work performed under Contract No. AT(45-1)-1350 between the Atomic Energy Commission and General Electric Company

Printed by/for the U. S. Atomic Energy Commission

Printed in USA. Price $1.00 Available from the
Office of Technical Services
Department of Commerce
Washington 25, D.C.

ABSTRACT

Thermal conductivity has been measured on several types of UO_2 specimens, both irradiated and nonirradiated. Variations in fabrication conditions can result in wide differences in thermal conductivity. High density, nonsintered, crystal compacts have a low, nearly temperature-independent conductivity while sintered polycrystalline UO_2 exhibits typical decreasing conductivity inversely proportional to temperature. Single crystals of UO_2 display increasing heat transfer rates at temperatures above 700 C, probably as a result of contributions by radiation and other energy transfer mechanisms.

Irradiation of sintered UO_2 at less than 100 C causes a decrease in thermal conductivity to 50% or less of its nonirradiated value near room temperature. As the temperature is raised, conductivity tends toward the corresponding nonirradiated values; pronounced stages of "recovery" occur near 150 C and 400 C, and less definitely near 800 C. This thermal annealing coincides with UO_2 crystal lattice parameter recovery, and appears to be associated with crystal lattice damage sustained during irradiation. Above 1000 C, no significant influence of irradiation on sintered polycrystalline UO_2 has been observed.

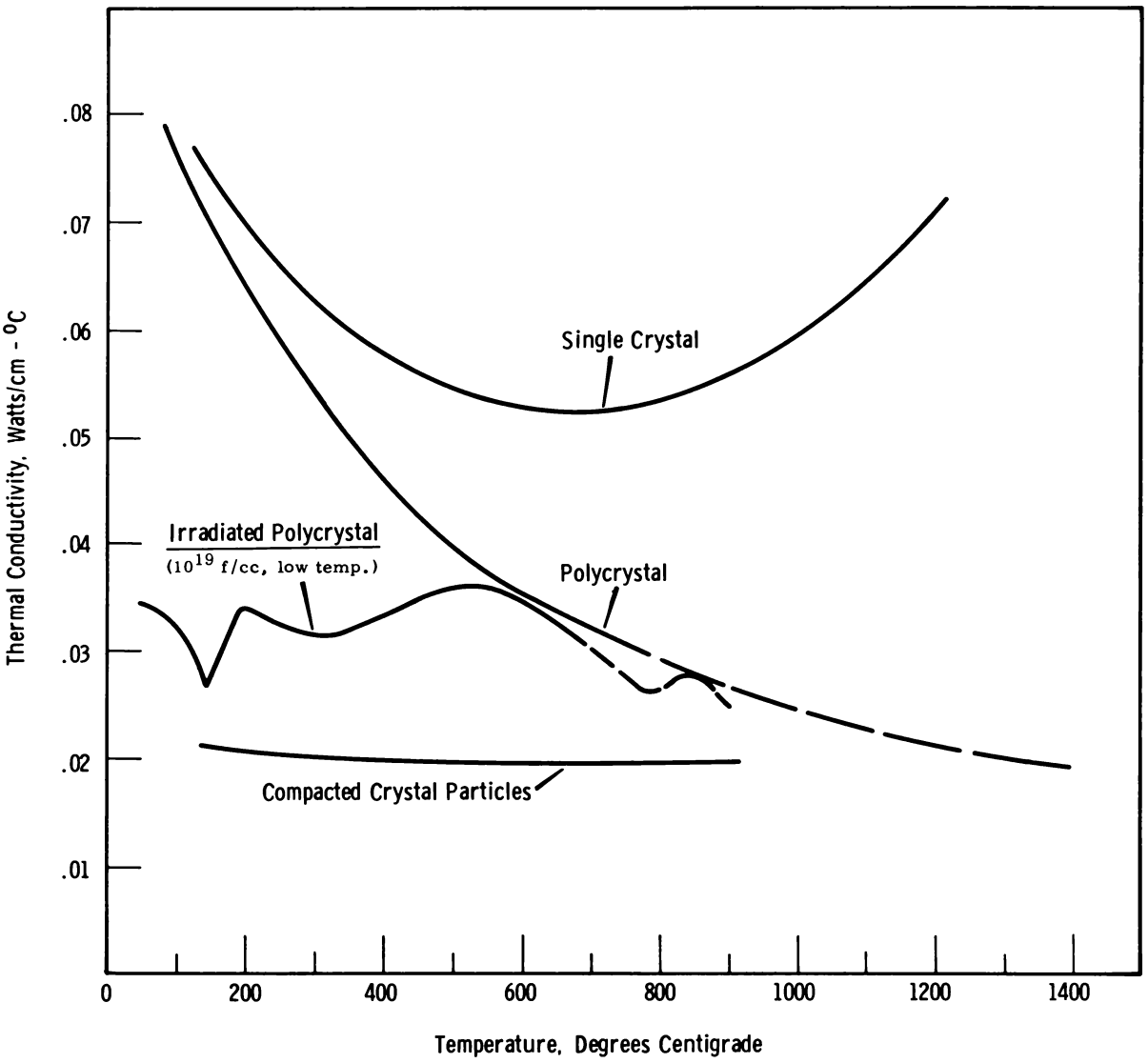

FIGURE i

Summary Curves: Thermal Conductivity of UO_2

AEC-GE RICHLAND, WASH.

TABLE OF CONTENTS

LIST OF FIGURES

THERMAL CONDUCTIVITY OF UO_2

INTRODUCTION

Thermal conductivity is one of the most important fundamental properties of uranium dioxide in connection with the use of UO_2 as a nuclear reactor fuel. The thermal conductivity influences the rate of energy transfer to the heat exchanger medium, the operating temperature of each point within the fuel, and consequently, the physical state of the materials present. At the same time, thermal conductivity is highly dependent on some of the same properties it influences most strongly. In addition, it has been shown that other more or less independent variables have a profound influence.[1] Particle and pore size, shape, distribution, and orientation[2, 3] play a significant role. Changes occur when other materials are present,[4, 5, 6] as deliberate additives, fission products, or contaminants. The presence of small amounts of additional oxygen in the uranium-oxygen lattice sharply reduces thermal conductivity.[2] Irradiation effects have been studied with in-reactor systems containing UO_2,[7] and in individual UO_2 specimens irradiated at not over 500 C.[2] Radiation was found to have a definite influence, although the basic nature and extent of this influence remained uncertain.

The present investigation was undertaken with two objectives in mind. First, what is the fundamental effect of irradiation on the thermal conductivity of UO_2, from near room temperature to the operating limit of UO_2; and second, what extremes of thermal conductivity might be encountered with various forms of high density UO_2 of possible interest for nuclear reactors? This paper reports the progress made to date in reaching those goals, through a cooperative program conducted by members of the Hanford Laboratories, General Electric Company, Richland, Washington, and the Instrumentation Division, Battelle Memorial Institute, Columbus, Ohio. Specimens were fabricated and irradiated, and supporting measurements and

examinations were made, in the Hanford Laboratories. Thermal and electrical measurements were made at Battelle using existing, adapted, and specially designed and built equipment.

Part I of this paper summarizes and discusses the thermal conductivity measurements, without elaboration on experimental details or data. Part II describes in more detail the sample preparation and measurement methods, and tabulates the data from which the curves were prepared. Electrical conductivity was determined on some of the thermal conductivity specimens. Those experiments and results are described elsewhere.[8]

PART I - THERMAL CONDUCTIVITY MEASUREMENTS AND RESULTS

A. Effect of Physical Form

As a reactor fuel, solid UO_2 is of interest in at least three different physical forms: compacted discrete particles, sintered polycrystalline shapes, and large single crystals. Under some conditions of reactor operation all three forms may exist simultaneously in each fuel element.[9] Overall thermal properties of the fuel then are established by the relative proportions and positions of each form. Nonirradiated specimens representing each of these forms (Table I) were used for the determination of thermal conductivity. All measured data were adjusted linearly to a comparison basis of 100% of theoretical density (zero porosity) using the simplified Loeb equation.[10]

1. Discrete Particles

The sample composed of compacted single crystal particles was contained in a thin-wall stainless steel cup. Proper selection of particle sizes and proportions, and vibration conditions, led to a bulk density of 87% of theoretical. Careful attention to experimental techniques assured accurate measurements of UO_2 thermal conductivity without interference from the container material.

The thermal conductivity of the compacted particles, Specimen E (Figures 1-a and 12), was found to be nearly constant between 150 and 900 C, within experimental error, similar to results reported for UO_2

TABLE I

NONIRRADIATED UO_2 THERMAL CONDUCTIVITY SPECIMENS

Specimen	Specimen Form	Density (Percent of Theoretical)	Oxygen/ Uranium Ratio	Fabrication Method
E-1	Particles in thin-wall shallow cup	86.8	2.002	*Vibrationally compacted single crystal particles
D(T)	Disk	92.9		Hydrostatically pressed, sintered
D(L)	Disk	93.2	2.006	Hydrostatically pressed, sintered
A	Disk	96.5		Die pressed, sintered
65	Cylindrical rod	87.1	2.002	Extruded, hydrostatically pressed, sintered
68	Cylindrical rod	91.7	2.002	Extruded, hydrostatically pressed, sintered
70	Cylindrical rod	95.3	2.002	Extruded, hydrostatically pressed, sintered
1000	Cylindrical rod	93.2	2.002	Hydrostatically pressed, sintered
G	Rectangular rod	99.4	2.003	Single crystal

* Approximate Composition:

+4 mesh	60%
-10 +20 mesh	30%
-35 +65 mesh	6%
-100 +200 mesh	4%

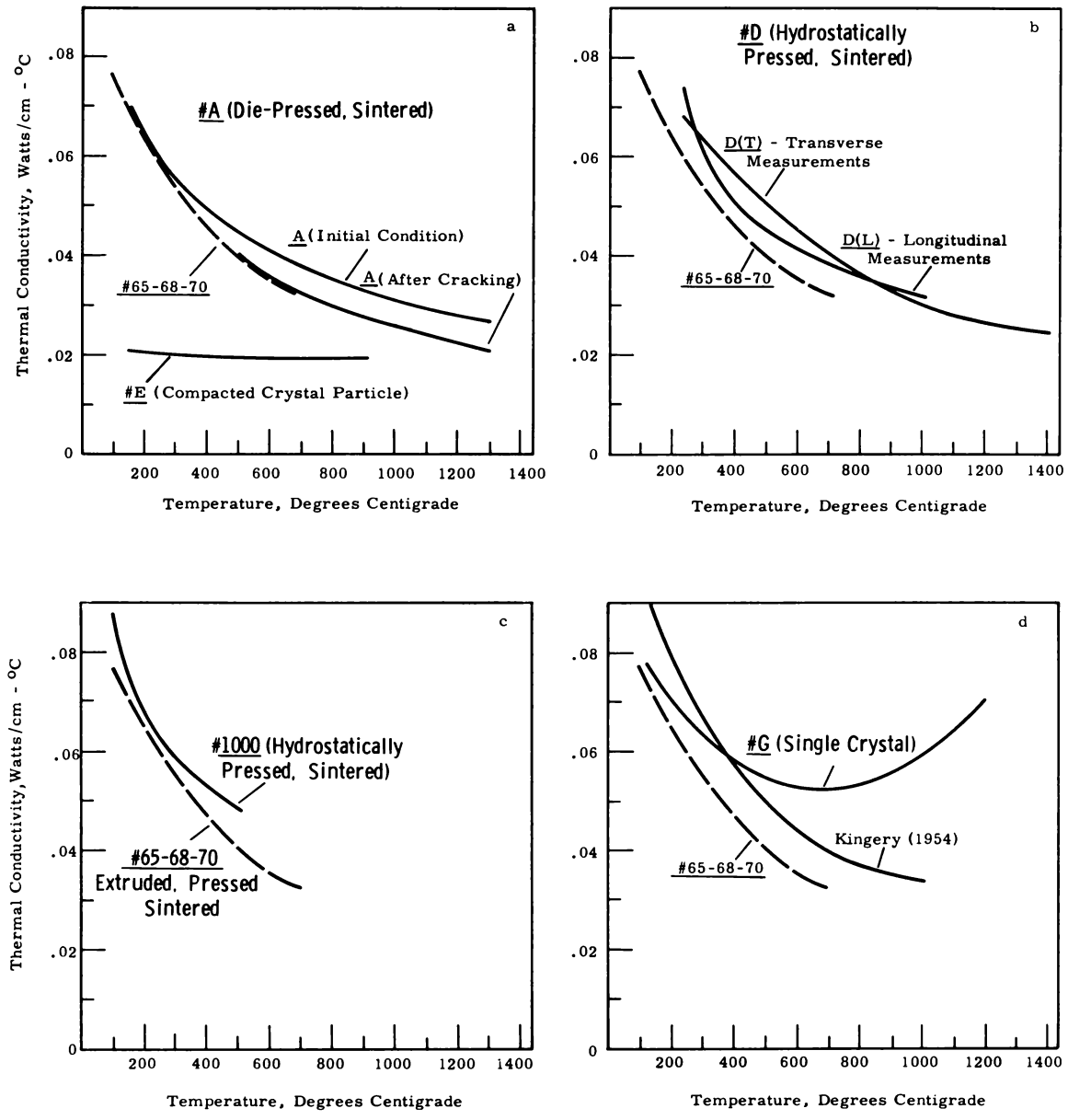

FIGURE 1

Effect of Physical Form and Fabrication Method on Thermal Conductivity of UO_2

powder[11, 12] and consistent with work reported by others[13, 14, 15] covering the range 600 to 2000 C. There was no significant difference between conductivity in helium and in argon atmospheres. It appears that the limiting factor, therefore, is the interfacial resistance between particles, rather than the UO_2 itself or the surrounding gas. If this is true, then the size, shape, and compact geometry of the specimen particles will exert a primary influence. The relationships shown in Figure 1-a may be considered representative of the conditions frequently used in vibrationally compacted elements.

2. Sintered Polycrystals

Thermal conductivity was measured on several sintered specimens representing various approaches to a similar product. All samples were sintered in hydrogen at 1650 to 1800 C.

The die-pressed disk, Specimen A, initially contained fine hairline cracks resulting from the fabrication method used; these could be expected to influence conductivity values (Figure 1-a and 12). Following measurements of Series 1 to over 1200 C, the sample was cooled to room temperature, and one of the cracks markedly widened. Subsequent measurements (Series 2) were shifted approximately 10% below the first series, probably due to the thermal resistance introduced by the widened crack.

Specimens D(T) and D(L) were obtained by machining disks, similar in shape to Specimen A, from adjacent sections near the center of a 20-inch sausage-shaped piece previously prepared by hydrostatic pressing and sintering. Specimen D(T) was cut with the disk axis (thermal measurement direction) transverse to the long axis of the original piece. The D(L) axis coincided with the long axis of the original piece. The specimens were free of defects, and none appeared during thermal measurements.

Figure 1-b and 13 show the thermal conductivity of the D specimens. Over the temperature range to 1100 C the difference between the two curves appears to be insignificant; the greater scatter of D(L) data is probably

due to thermocouple error. It can be concluded that thermal conductivity of these pieces shows no significant dependence on the direction of measurement.

A cylindrical specimen, 1/4-inch diameter by 3-inches long, was also prepared by the same procedure as used for the D specimens, using another hydrostatically pressed and sintered piece. Conductivity was measured on the apparatus designed and used for irradiated specimens. The thermal conductivity of the resulting specimen #1000 (Figure 1-c and 14) was slightly lower than that of the disk specimens D, but similar in all other respects.

On the other hand, similar 1/4-inch cylindrical specimens (#65, 68, and 70) prepared by first extruding to near final size and shape, followed by hydrostatic pressing and sintering, had a thermal conductivity over 10% lower than #1000 (Figure 1-c and 14). Examination of the microstructure of these latter specimens (Figure 2) suggests that the conductivity difference is related to the size, shape, and distribution of pores and/or grain boundaries.

It is interesting to compare the present data with that of previous investigators. The work by Kingery[16] is most frequently quoted; it should be noted that the Kingery data were obtained from a UO_2 sample of 73% theoretical density, and require a relatively large correction to the zero porosity basis. Figure 1-d shows that the curve shapes and slopes are generally similar, and thermal conductivity values for all polycrystalline samples are within about ±10% of their average at temperatures up to 1000 C. Considering the variety of sample preparation methods and starting materials, this is considered to be very satisfactory agreement.

3. Single Crystals

A large single crystal was selected from UO_2 prepared by the commercial arc-fusion process. The crystal was imperfect, and contained some inclusions, defects, and low-angle boundaries (Figure 3). However, X-ray diffraction examination of similar pieces confirmed single crystal

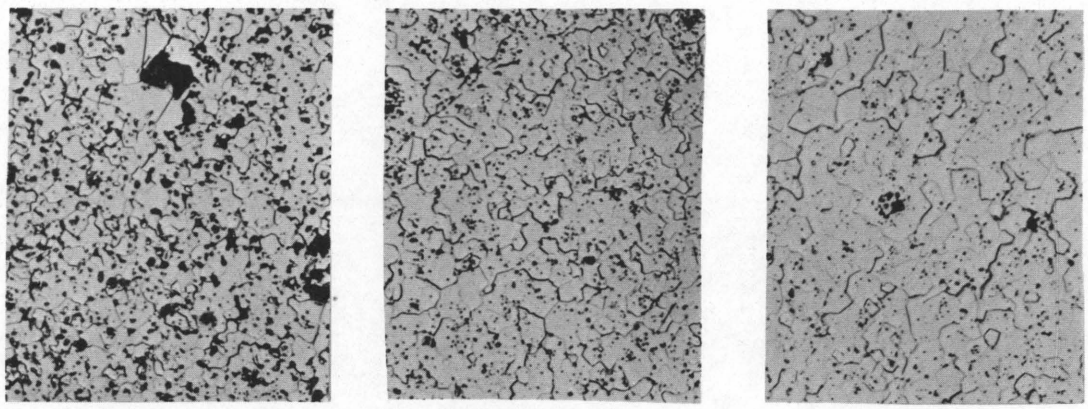

Specimen 65
87.1% TD

Specimen 68
91.7% TD

Specimen 70
95.3% TD

a. Extruded, Hydrostatically Pressed, Sintered

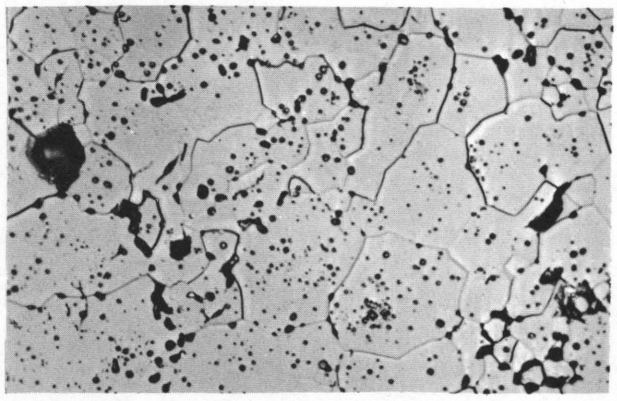

Specimen 1000
93.2% TD

b. Hydrostatically Pressed, Sintered

FIGURE 2

Microstructure of Sintered Thermal Conductivity Specimens (500 X)

AEC-GE RICHLAND, WASH.

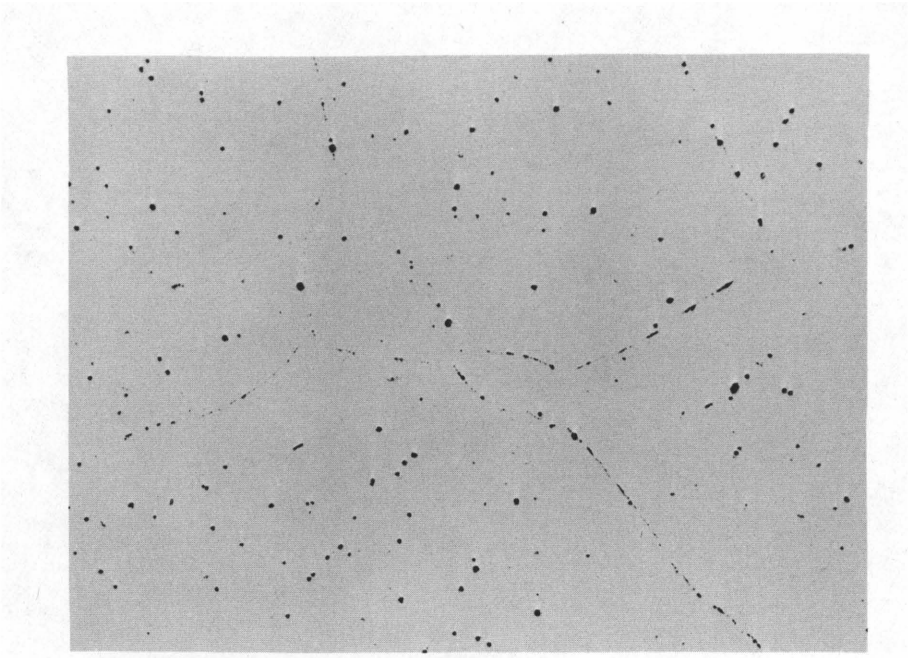

a(100 X)

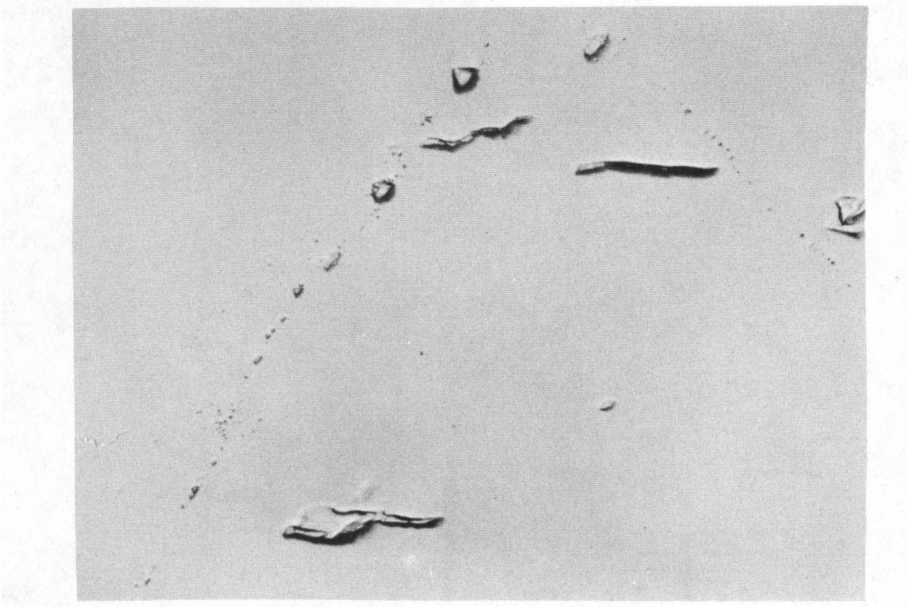

b(500 X)

FIGURE 3

Microstructure of Single Crystal UO_2
Thermal Conductivity Specimen

AEC-GE RICHLAND, WASH.

structure for their entire length. The crystal (#G) used for conductivity measurements was ground to a rectangular cross section, and one side polished and chemically etched for metallography. Holes were drilled ultrasonically for thermocouples and guide pins.

Thermal conductivity of the single crystal near room temperature was approximately the same as for sintered UO_2 (Figures 1-d and 15). However, with rising temperature the conductivity remained well above that for sintered material; at 700 C it was 60% higher than the average sintered UO_2 value at that temperature. With further temperature rise the thermal conductivity increased, so that at 1200 C it was approximately the same as at 200 C. The curve shape suggests a significant contribution by a thermal radiation process in addition to the conduction component, and confirms earlier predictions in work by Bates.[17] Recent higher temperature work with sintered pellets under simulated reactor thermal conditions[13, 14] also indicates increasing thermal conductivity at elevated temperatures.

B. Irradiation Effects

Although it had been established previously that reactor irradiation has an effect on UO_2 thermal conductivity, there still remained considerable question regarding the extent of this effect, the conditions under which it occurs, and the basic changes occurring in the UO_2 leading to the observed thermal conductivity behavior upon irradiation. In order to shed light on these questions, the following experimental approach was followed.

About 100 sintered UO_2 specimens were prepared, all as nearly identical as possible except for deliberate variations in bulk density between 86 and 96% of theoretical. Some of these pieces served as nonirradiated controls; thermal conductivity measurements on three of them (#65, 68, and 70) were discussed above (Section A-2). Other pieces were inserted in a low-flux position of a Hanford reactor and kept there for sufficient time to accumulate exposures ranging from 1.4 to 10^{18} to more than 10^{19} f/cc. The maximum temperature of the specimens is calculated to have been less than 100 C, and probably less than 60 C. (Table II)

TABLE II

IRRADIATED UO_2 THERMAL CONDUCTIVITY SPECIMENS

Specimen	Specimen Form	Density Percent of Theoretical	Fabrication Method	Irradiation f/cc
11	Cylindrical rod	91.8	Extruded, hydrostatically pressed, sintered	1.4×10^{18}
19	Cylindrical rod	94.1	Extruded, hydrostatically pressed, sintered	4.1×10^{18}
51	Cylindrical rod	94.5	Extruded, hydrostatically pressed, sintered	1.1×10^{19}

Following removal from reactor the specimens were separated from their containment capsules, and representative pieces used for conductivity measurements, burn-up analyses, metallographic examinations, annealing studies, and other tests. Some of that work is still in progress. Measurements of the sintered UO_2 thermal conductivity were made using the equipment especially designed for this work. About 24 hours elapsed between successive measurements, allowing time for thermal equilibration and annealing of temperature-dependent effects of irradiation.

Data and curves for thermal conductivity at three radiation exposure levels are shown in Figure 4, and Figures 15, 16, and 17. The curve for the corresponding nonirradiated specimens is included in Figure 4 for comparison. The numbered arrows on the curves indicate successive heating and cooling cycles during measurements. Several features of these curves are particularly noteworthy.

1. Irradiation to 10^{18} f/cc or more reduces the room temperature thermal conductivity by 50% or more. No saturation was found up to 1.1×10^{19} f/cc, following irradiation at temperatures below 100 C.

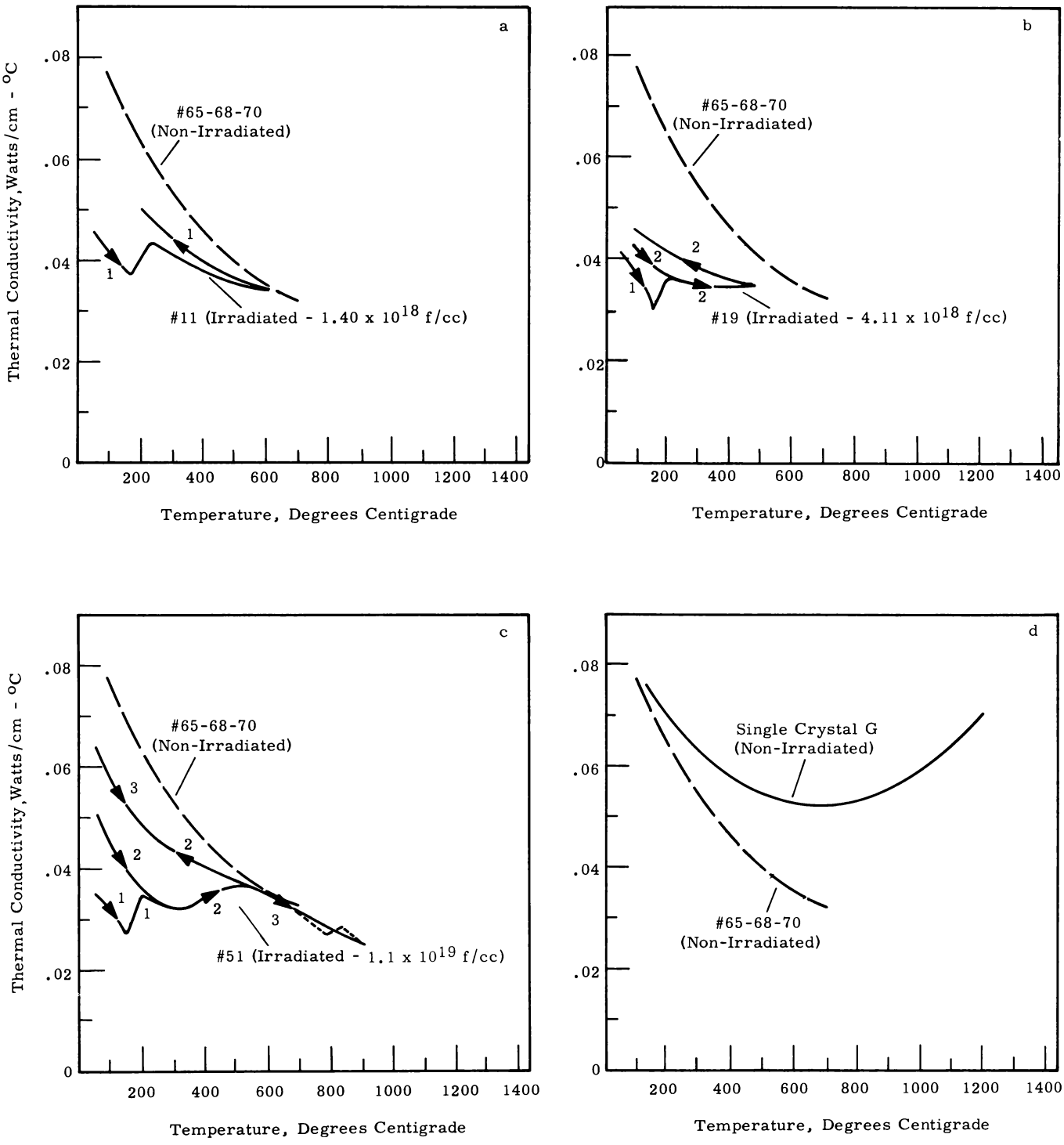

FIGURE 4

Effect of Low Temperature Irradiation on Thermal Conductivity of Sintered UO_2
(Maximum UO_2 temperature during irradiation, <100 C)

AEC-GE RICHLAND, WASH.

2. Thermal conductivity of irradiated sintered UO_2 decreases initially in a normal manner with increasing temperature. The first point of inflection is reached at 150 - 200 C, the conductivity abruptly increasing about 20% (0.008 watts/cm-°C). The amount of increase is independent of the radiation exposure of the UO_2, but occurs at a lower temperature with increasing exposures.

3. Further temperature increase again causes a normal decrease in thermal conductivity, until a second point of rise is encountered, at about 350 - 400 C. This increase is not as sharp as the first at lower temperature, and appears proportional to the radiation exposure of the UO_2.

4. A third point of inflection is suggested by the data for the 1.1×10^{19} f/cc sample, at about 800 C. However, the shape of the curve in that region is uncertain because of the limited number and precision of data. Work is continuing to clarify that point.

5. If the sample is cooled after reaching any temperature during the initial rise, the thermal conductivity curve at all lower temperatures assumes the normal shape and slope, displaced downward to join the initial (irradiated) curve at the highest temperature reached previously.

6. The extent of recovery from the original irradiated conductivity value to the nonirradiated level is dependent on the maximum temperature to which the material has been subjected during or after irradiation, and on the temperature of measurement. (Recovery of sample #51, 1.1×10^{19} f/cc, appeared to be over 90% at 900 C; subsequent room temperature measurements have not yet been completed.)

The single crystal specimen (#G) on which thermal conductivity measurements were made was subsequently irradiated to about 10^{14} f/cc, at a temperature below 325 C. Measurements then were made with the same equipment used for the earlier thermal measurements on the non-irradiated crystal.

Resulting apparent thermal conductivity was 5 to 20% lower than the corresponding nonirradiated values. This relatively large reduction in conductivity following low-level irradiation cannot be explained by comparison with behavior of sintered UO_2. It is possible that physical damage to the crystal structure may have occurred, due to thermal or other irradiation effects, sufficient to interfere with the "ideal" heat transfer mechanism shown before irradiation. However, no evidence of microcracking has been resolved in optical micrographs to 500 X. Further irradiations, measurements and examination of the single crystal are in progress.

C. Discussion and Conclusions

It is apparent that nonirradiated UO_2 thermal conductivity values within a wide range may be obtained by proper choice of starting materials and specimen preparation technique. Actually, the method and materials are not as significant as the combination of conditions under which they are used, and the basic effect on physical characteristics of the resulting piece. Even within a general type such as sintered compacts, significant variations can be introduced by changes in one or more conditions. These factors appear mainly responsible for the wide range of thermal conductivity values for UO_2 reported in the literature.[1, 11, 12, 14, 15, 16, 18, 19] Unless all pertinent variables are recognized and controlled, no sound basis exists for direct comparison of absolute values.

The upturn in the single crystal curve agrees reasonably well with the curve derived by combination of a conduction component (1/T dependence) and a radiation component (T^3 dependence). Bates has shown recently[20] that a better curve fit to the experimental data may be obtained by inclusion of a third component based on an excitation process. Exact agreement would not be expected, because of the uncertain contributions by electronic energy transfer, specimen boundary interactions influencing photon conductivity, and the increase in photon effective mean-free-path at higher temperatures.[21]

It is clear that irradiation tends to depress thermal conductivity. The foregoing data, showing the occurrence of two distinct stages of recovery of sintered UO_2 from radiation damage, and suggesting existence of a third stage, are in substantial agreement with conclusions reached by Ross,[2] based on somewhat different evidence. There is also good correlation here with the irradiation-induced changes in UO_2 lattice dimensions, as measured by Bloch.[22] In that work, uranium dioxide showed a relative variation in crystal parameter of 8.6×10^{-4} upon low temperature irradiation to 1.5×10^{17} f/cc. The curve shown in Figure 5 resulted from subsequent annealing in vacuum. The steps in lattice recovery correspond to within ±50 C with steps in the present thermal conductivity recovery curves.

Although no saturation was found, up to 1×10^{19} f/cc, for radiation-induced reduction of thermal conductivity measured below 150 C, this observation is not necessarily in conflict with that of Ross. The saturation point would be expected to depend very greatly on irradiation temperature. The lower limit found by Ross may have been imposed by his higher temperature of irradiation, leading to minimum values corresponding to positions beyond the first break in the present curves. The Ross data do show an increase in the temperature stability of the conductivity change as irradiation increases, apparently due to the increasing influence of the high temperature end of the curve. It must be noted that Bloch found no further lattice dimension changes for irradiation greater than 2×10^{17} f/cc, with a bulk irradiation temperature of < 62 C.

The decrease in thermal conductivity upon irradiation is much greater than would be caused by reasonable changes in stoichiometry. In addition, the lattice parameter changes observed by Bloch were opposite to that which would be caused by oxidation. Fission product concentration is very low at these irradiation levels, and would not be expected to exert an appreciable influence.

It appears evident, therefore, that the thermal conductivity changes are a result of point defects or other lattice damage sustained during irradiation. A mechanism is indicated leading to the existence of three distinct

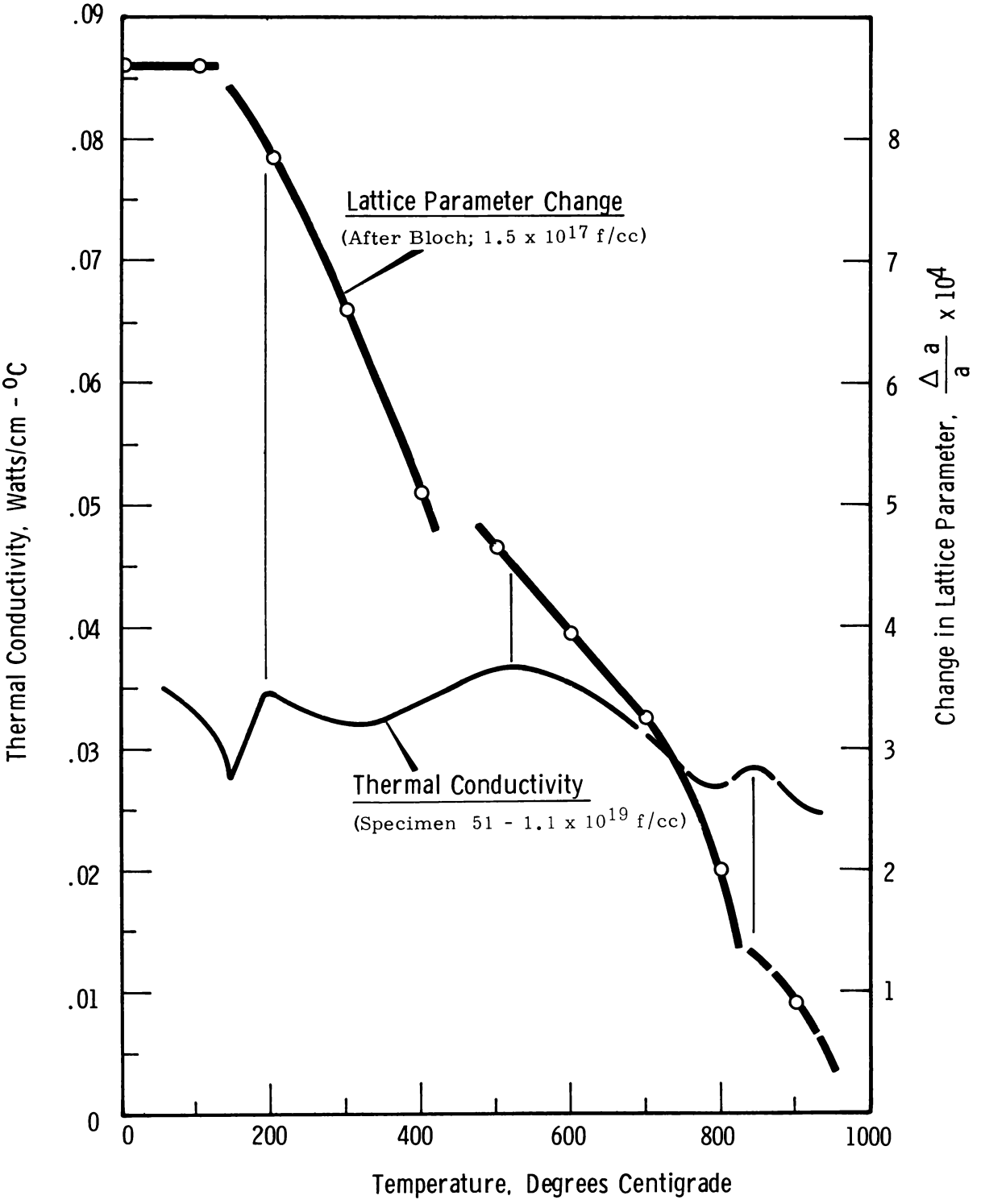

FIGURE 5

Thermal Annealing of Irradiated Sintered UO_2
(Maximum UO_2 temperature during irradiation, <100 C)

AEC-GE RICHLAND, WASH.

components of damage, the proportions of which are dependent on temperature and irradiation conditions. Further study is needed to determine the mechanism details.

D. Acknowledgements

The authors gratefully acknowledge the considerable assistance of many members of the Ceramics Research and Development Operation of the Hanford Laboratories; the discussions and assistance of J. Lambert Bates have been particularly helpful. The authors are also indebted to members of the Hanford Radiometallurgy Laboratory where the preparation and examination of radioactive specimens were carried out, and to the members of the Physical Measurements Group, Instrumentation Division of Battelle, for their valued assistance in making thermal property measurements.

PART II - EXPERIMENTAL DETAILS AND DATA

A. Fabrication of Specimens

The sintered UO_2 specimens were prepared from high-purity UO_2 powder, by two different methods. The 1/4-inch diameter rods (except specimen #1000) were extruded, hydrostatically pressed, sintered, and ground to final dimensions. Specimen #1000 and the disk specimens were machined from larger compacts prepared by hydrostatic or die pressing and sintering (Figure 6-a).

The single crystal particles, specimen E-1, were vibrationally compacted in a stainless steel cup of the same size and shape as the disk specimens. Particle sizes were chosen to give maximum packed density. The large single crystal specimen was prepared by grinding from a selected boule obtained by a commercial arc fusion process (Figure 6-b).

The methods of preparation of the individual samples are indicated with the data and curves of Figures 12 to 17 (fold-out sheets). In all sample preparation, details of fabrication procedures were adjusted to achieve control over sizes, shapes, and densities of samples.

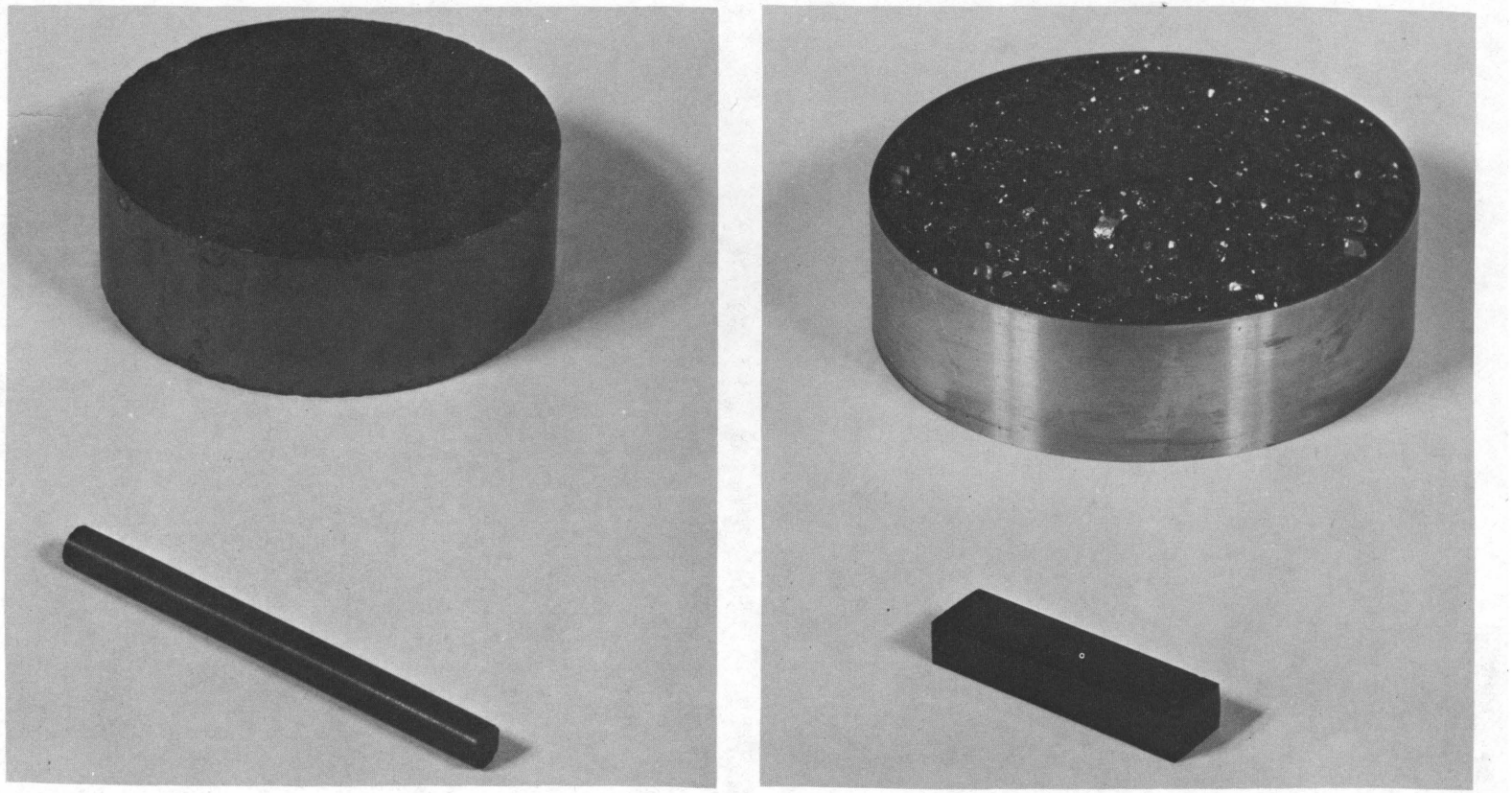

a - Pressed and Sintered UO_2

b - UO_2 Crystals
(Upper: Compacted Crystal Particles
Lower: Single Crystal)

FIGURE 6

UO_2 Thermal Conductivity Specimens (Approximately actual size)

B. Irradiation of Specimens

Irradiations were conducted in Hanford reactors, for exposure times up to 4 years. The 1/4-inch by 3-inches sintered UO_2 rods were placed in irradiation capsules of the type shown in Figure 7. Two of the samples in each capsule were notched around the circumference midway between the ends to facilitate later use as fractography specimens. Two samples of each density range ("low" 86 - 88% theoretical; "medium", 90 - 93%; and "high", >93%) completed the loading of eight specimens per capsule. Capsules were closed by inert gas shielded arc welding, after filling void spaces with helium. Irradiation rate was selected to maintain the maximum sample temperature below 100 C; the estimated internal temperature of specimens was 60 C. Capsules were removed from the reactor at selected intervals, and UO_2 specimens removed from the capsules using the Hanford Laboratories Radiometallurgy facilities.

The large single crystal was irradiated after encapsulation as shown in Figure 8. Irradiation was conducted in the Hanford Snout facility, which could be used for minimum total irradiations on the order of 10^{14} f/cc. Sample temperature during the irradiation was less than 325 C.

Individual irradiation levels for each sample are shown with the data and curves on Figures 12 to 17.

C. Measurement of Thermal Conductivity

Criteria for evaluation of several basic methods of measurement of thermal conductivity were well established at the time this investigation began.[23, 24] New methods reported since then include at least one well suited for dynamic studies on small samples.[25]

In the present work, the variety of UO_2 sample types made it necessary to use several different methods and sets of equipment. Data were correlated by duplicate measurements of the same or similar samples on different instruments, and by calibration with appropriate standards. Calibration materials included clear fused quartz, a titanium alloy of

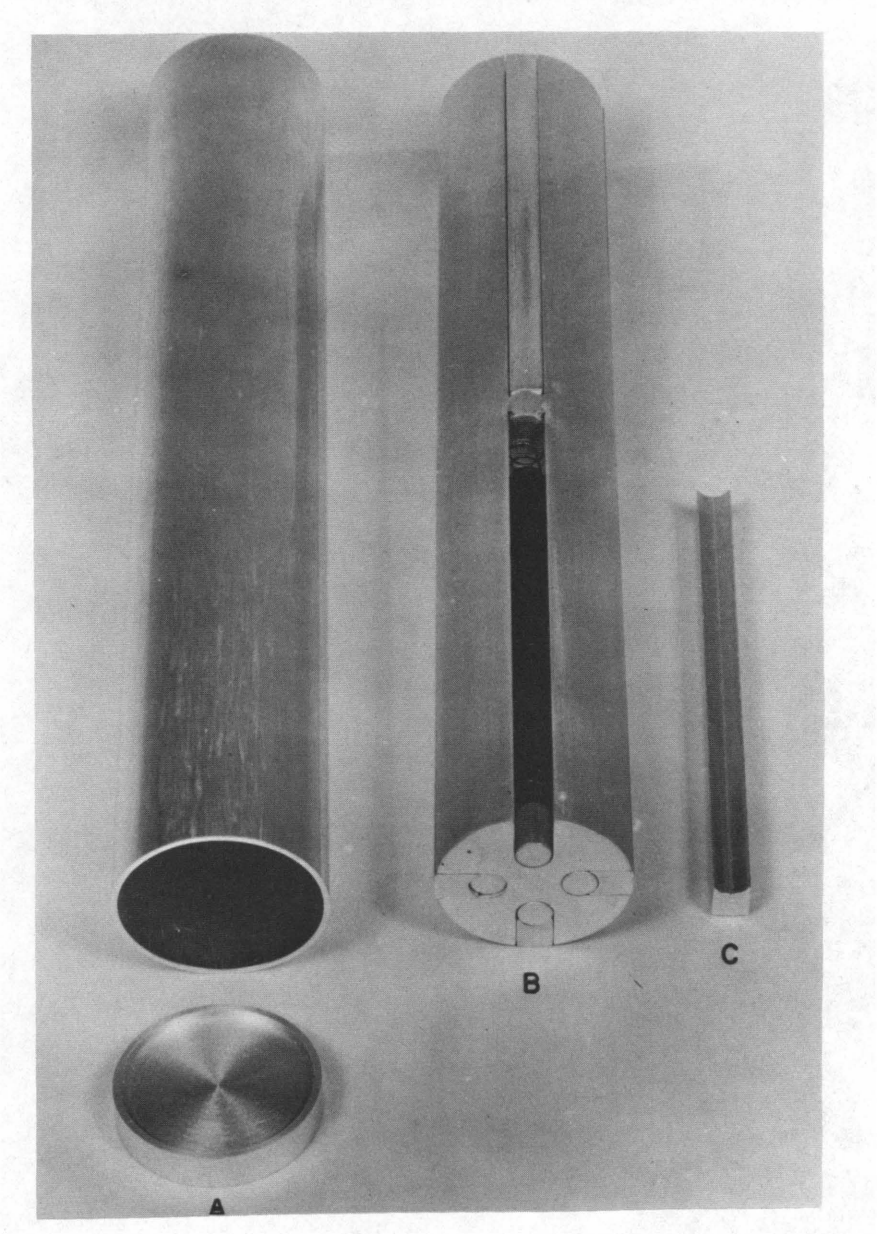

FIGURE 7

Irradiation Capsule for Sintered UO_2 Rods
(Approximately half size)

AEC-GE RICHLAND, WASH.

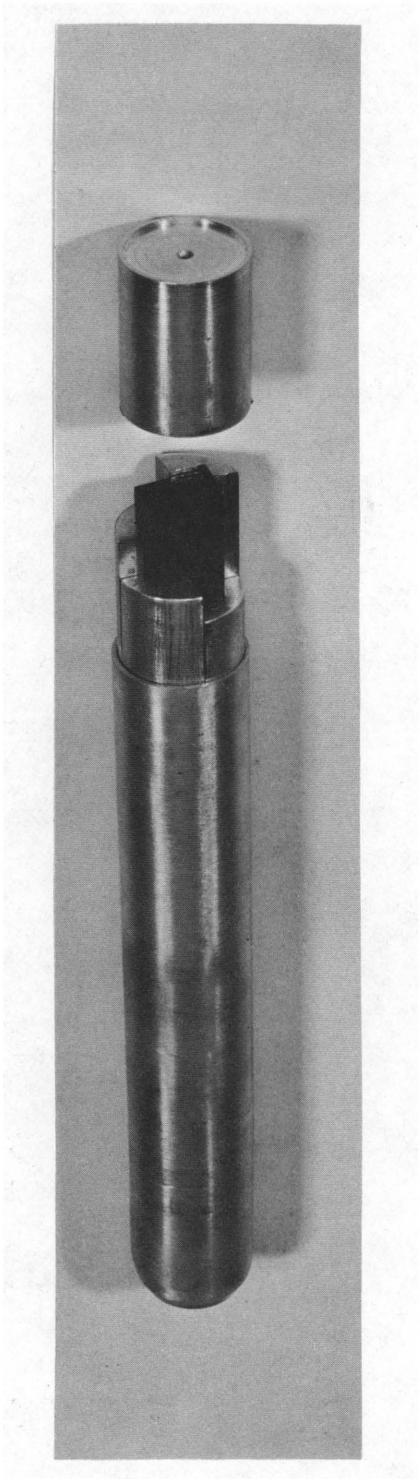

FIGURE 8
Irradiation Capsule
for UO_2 Single Crystal
(Approximately 3/4 actual size)

AEC-GE RICHLAND, WASH.

6 wt% aluminum - 4 wt% vanadium, Type 347 stainless steel, Armco iron, and zirconia.

1. Specimens A, D(T), D(L), E-1

The disk-shaped specimens were measured on existing Battelle equipment, shown in Figure 9. The apparatus is based on a steady-state, comparative, longitudinal heat flow method. To maintain uniform heat flux through the apparatus, a layer of carbon cloth was used between the heat leveling block and sample, and a silica-fiber cloth between sample and heat-flow meter. All solid disk specimens were measured in an argon gas atmosphere; Specimen E (compacted particles) was measured both in argon and in helium.

The compacted particles contained in a stainless steel cup (Specimen E-1) was treated as a disk specimen. During measurements, special attention was given to determination of effects of outer guard cylinder temperature changes; stability of specimen temperature indicates that presence of the steel cup had no measurable effect on thermal conductivity data obtained.

2. Specimens 65, 68, 70, 1000, 11, 19, 51

The apparatus used for the 1/4-inch cylindrical specimens, Figure 10, was designed and built specifically for this work, based on the specimen geometry required for satisfactory irradiation conditions. The absolute steady-state method was selected because it has a demonstrated reliability, is capable of the necessary accuracy, and yields conductivity directly from the measurements. Careful attention was paid to guarding the heater so that all heat generated went into the specimen, and to preventing heat losses through thermocouples and other components. Temperatures were measured by positioned miniaturized compensated thermocouples. Specimens were held in vacuum of about 2×10^{-5} mm mercury during measurements.

3. Specimen G

The single crystal measurements were made by the steady heat flow comparative method of Van Dusen and Shelton.[26] The apparatus (Figure 11) including an encircling guard tube, in which temperatures were adjusted at

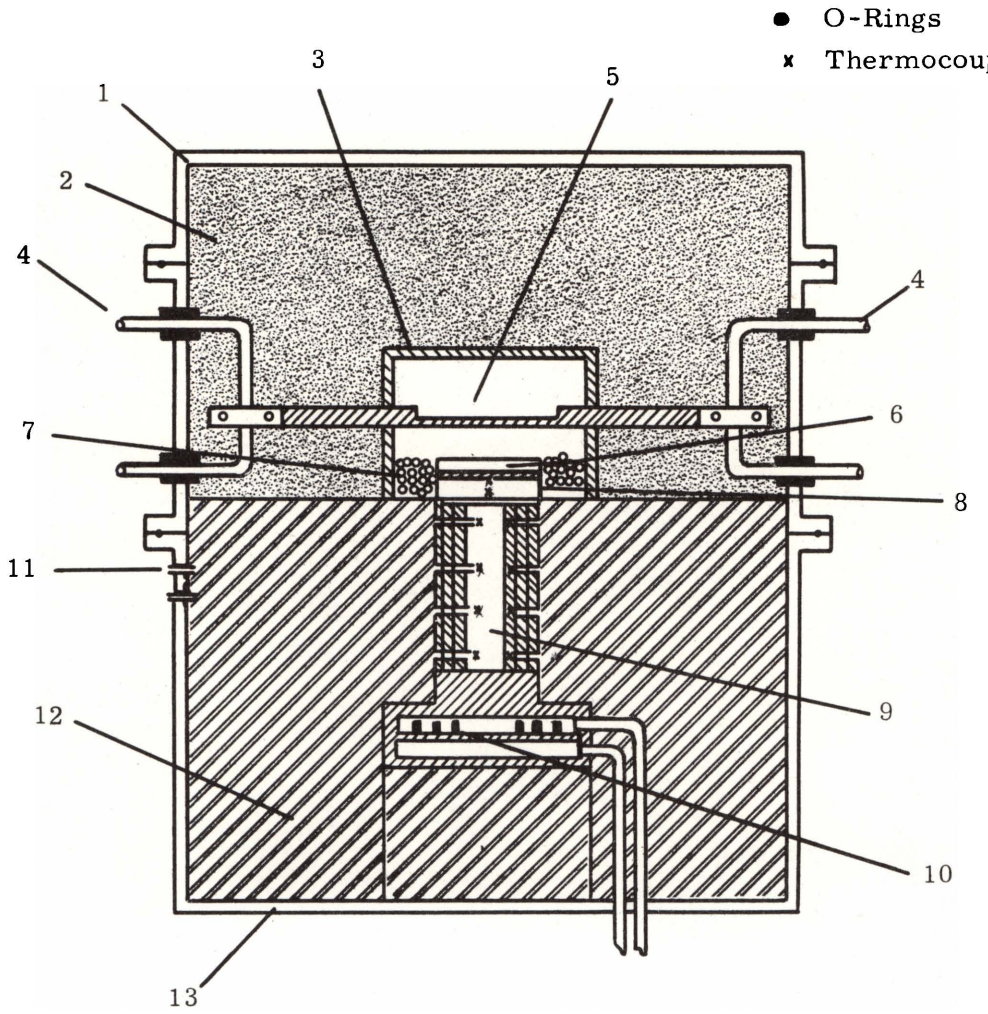

1. Container Top
2. High-Temperature Insulation, K-30 Brick in Cooler Region and E-163 Grain Al_2O_3 in Hotter Region
3. Zirconia Shield
4. High-Current Electrode Assembly
5. Graphite Heater
6. Graphite Heat-Leveling Block
7. High-Temperature Insulation, E-163 Grain Al_2O_3
8. Specimen
9. Heat-Flow Meter Assembly
10. Heat Sink
11. Hermetic Seals
12. Insulation, K-30 Brick
13. Container

FIGURE 9

Thermal Conductivity Apparatus for Disk Specimens

AEC-GE RICHLAND, WASH.

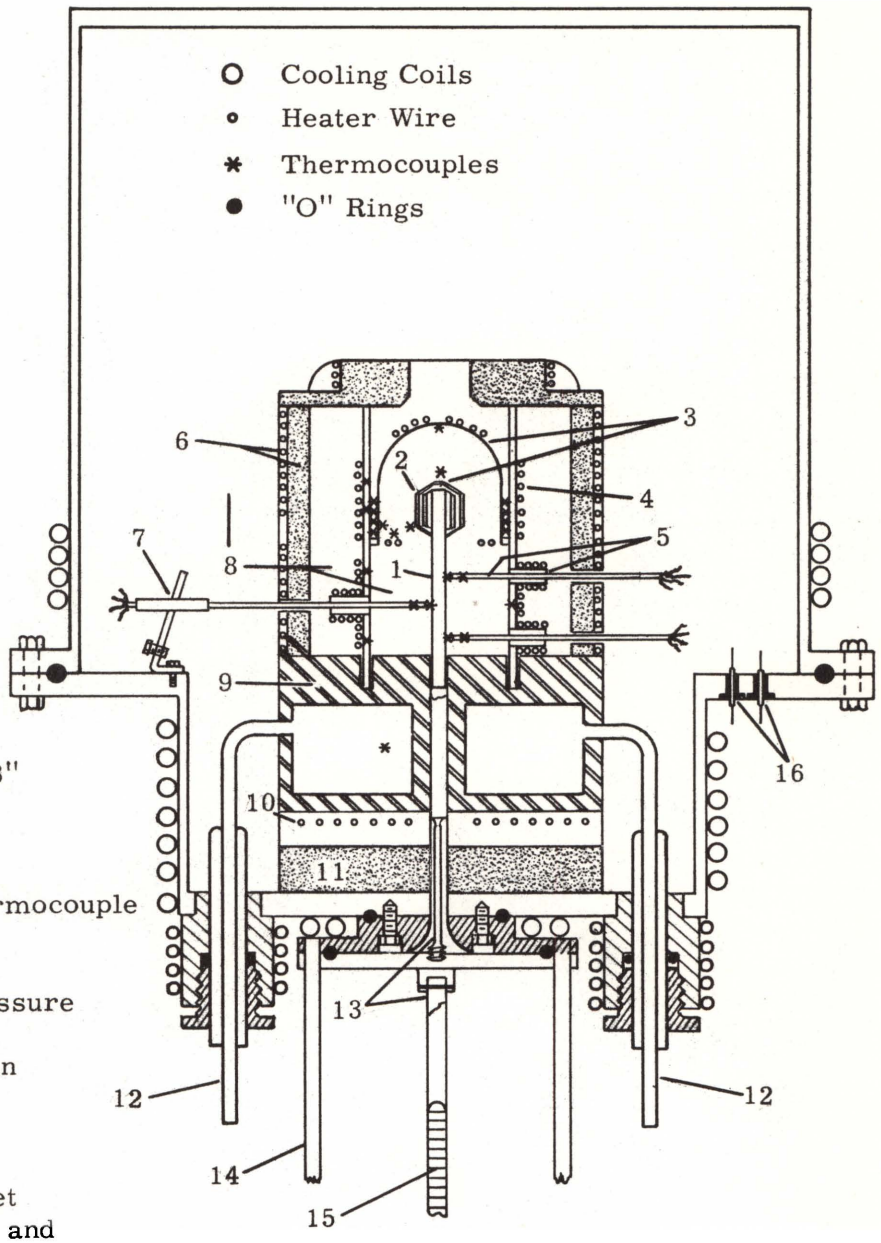

1. Specimen, 1/4" x 3"
2. Specimen Heater
3. Heater Shields
4. Guard
5. Compensating Thermocouple Assembly (3)
6. Outside Heater
7. Thermocouple Pressure Spring and Guide
8. Fiberfrax Insulation
9. Sink
10. Sink Heater
11. Insulation
12. Sink Inlet and Outlet
13. Specimen Pedestal and Lift Assembly
14. Lift Guides (3)
15. Lift Rack-Gear Driven
16. Hermetic Seals

FIGURE 10

Thermal Conductivity Apparatus for 1/4-Inch Diameter Cylindrical Specimens

AEC-GE RICHLAND, WASH.

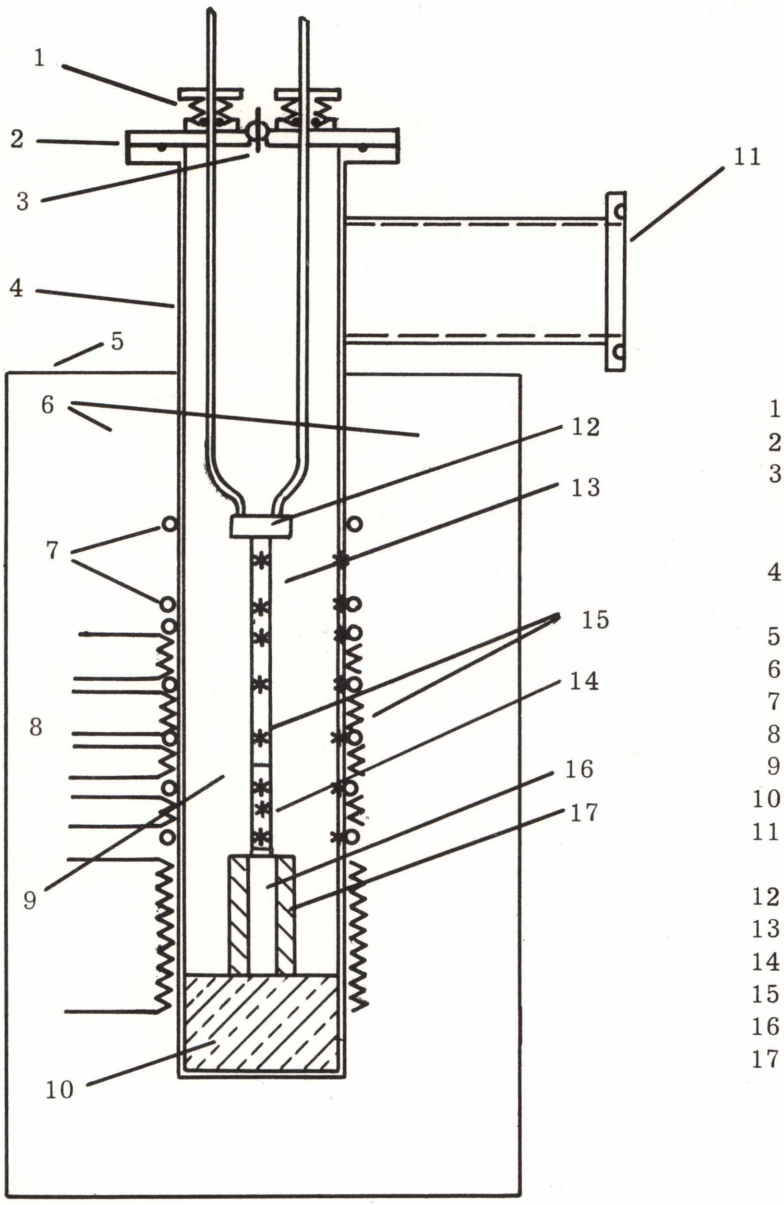

1. Vacuum Seals
2. Top Plate
3. Hermetic Seals for Thermocouples and Power Leads
4. Vacuum Chamber and Guard
5. Insulation Enclosure
6. Sil-O-Cel Insulation
7. Guard Cooling Coils
8. Guard Balancing Heaters
9. Insulation
10. K-30 Brick
11. Connection to Vacuum System
12. Sink Assembly
13. Reference Standard
14. Specimen
15. Thermocouples*
16. Heater Block
17. Specimen Heater

FIGURE 11

Thermal Conductivity Apparatus for Rectangular Rod Specimens

AEC-GE RICHLAND, WASH.

steady state to match those of specimen and standard at corresponding levels. A vacuum of about 2×10^{-5} mm mercury was maintained during measurements. Two similar sets of apparatus were used during the course of work on Specimen G; good agreement was obtained between data determined with each.

D. Curves and Data

The detailed curves for all samples, the data from which the curves were prepared, and a brief summary of fabrication and experimental treatment appear on the following pages. All data are "as measured" values adjusted to a common basis of zero porosity (100% theoretical density, TD) by application of the simplified Loeb equation.[10] Measurements are considered accurate to ±5% unless otherwise indicated with the data.

The curves are shown on the fold-out half of each page, to allow convenient comparison by overlaying sheets of particular interest. The same scale has been used for all curves in this section. The curve for the nonirradiated single crystal appears on each page for comparison, and to assist in correctly aligning the axes.

SPECIMEN A - DISK

Nonirradiated UO_2
Die pressed, sintered

Length 2.256 cm
Diameter 7.513 cm
Weight 1055.0 g
Density 10.59 g/cc (96.5% TD)

Measured Data

Series 1

	Temperature °C	Thermal Conductivity watts/(cm)(° C)
Run 1	273	0.0542
	293	0.0535
	397	0.0487
	432	0.0447
Run 2	401	0.0469
	604	0.0392
	808	0.0326
	884	0.0337
	918	0.0299
	1035	0.0256
	1062	0.0248
Run 3	130	0.0727
	140	0.0711
	256	0.0588
	263	0.0598
	277	0.0565
	285	0.0584
	349	0.0542
	361	0.0520
	380	0.0520
	388	0.0516
	476	0.0480
	517	0.0460
	692	0.0382
	749	0.0386
	998	0.0337
	1120	0.0284
	1134	0.0306
	1233	0.0264
	1279	0.0314
Series 2		
	474	0.0403
	530	0.0397
	738	0.0292
	830	0.0297
	947	0.0258
	1098	0.0256
	1119	0.0236
	1151	0.0236
	1341	0.0218

SPECIMEN E-1 - DISK

Nonirradiated UO_2

Vibrationally compacted particles of fused UO_2 contained in stainless steel cup (wall thickness 0.029 inch).

Length 2.502 cm
Diameter 8.738 cm
Weight 1428.0 g
Density 9.52 g/cc (86.8% TD)

Measured Data

Series 1

Argon Atmosphere

Temperature °C	Thermal Conductivity watts/(cm)(°C)
188	0.0207
281	0.0167
310	0.0204
397	0.0204
672	0.0161
690	0.0199
888	0.0205

Series 2

Helium Atmosphere

Temperature °C	Thermal Conductivity watts/(cm)(°C)
151	0.0212
364	0.0199
474	0.0181
707	0.0157
772	0.0311
796	0.0152
895	0.0308

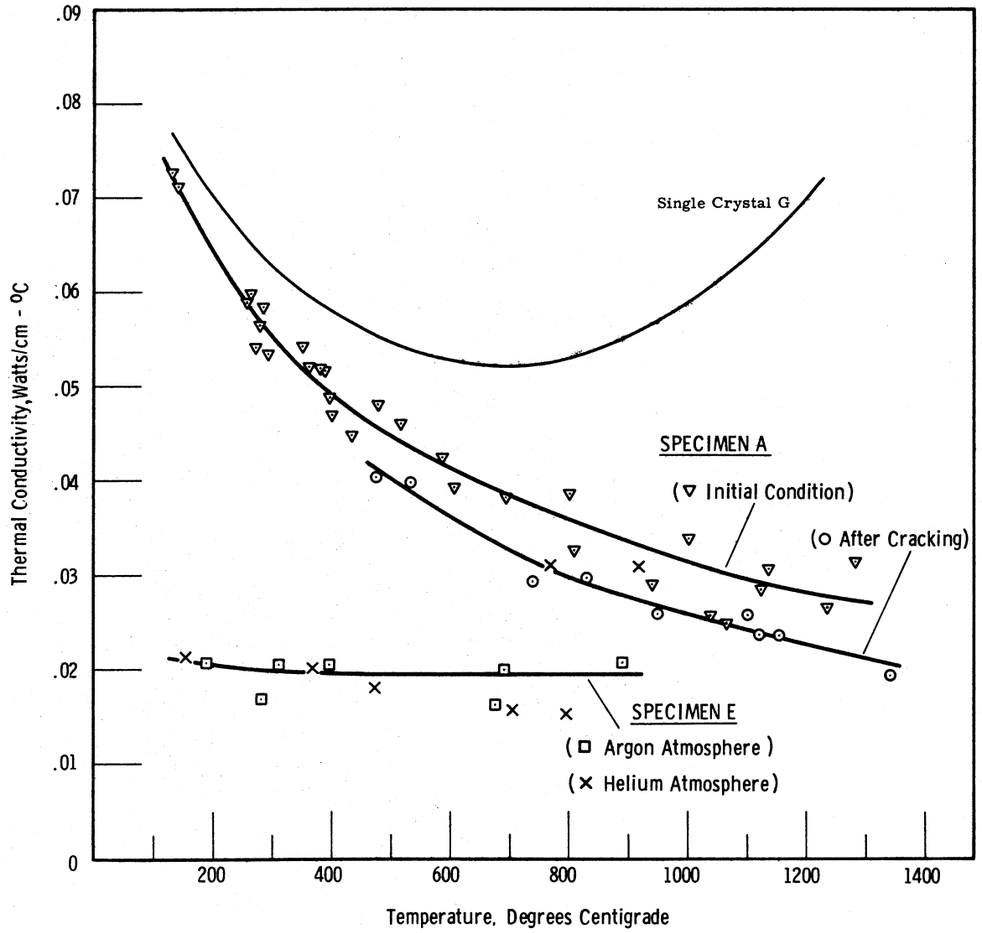

FIGURE 12

Thermal Conductivity of UO_2
(Die Pressed and Sintered; Compacted Particles)

AEC-GE RICHLAND, WASH.

SPECIMENS D - DISKS

Nonirradiated UO_2

Machined from large hydrostatically pressed and sintered piece.

SPECIMEN D(L)

Disk axis coincides with long axis of original piece.
Edges chipped.

Length	2.222 cm
Diameter	7.600 cm
Weight	983.3 g
Density	10.22 g/cc (93.2% TD)

Measured Data

Temperature °C	Thermal Conductivity watts/(cm)(° C)
253	0.0706
269	0.0579
275	0.0733
292	0.0632
419	0.0549
460	0.0472
548	0.0389
614	0.0405
724	0.0325
779	0.0426
779	0.0374
899	0.0373
899	0.0295
1044	0.0296

SPECIMEN D(T)

Disk axis perpendicular to long axis of original piece.

Length	2.222 cm
Diameter	7.104 cm
Weight	897.3 g
Density	10.19 g/cc (92.9% TD)

Measured Data

Temperature °C	Thermal Conductivity watts/(cm)(°C)
241	0.0692
365	0.0513
373	0.0591
397	0.0608
490	0.0461
542	0.0505
570	0.0434
632	0.0423
637	0.0430
672	0.0386
706	0.0438
713	0.0400
764	0.0383
822	0.0354
937	0.0304
955	0.0320
1064	0.0292
1086	0.0282
1112	0.0291
1166	0.0268
1176	0.0286
1135	0.0251
1432	0.0233

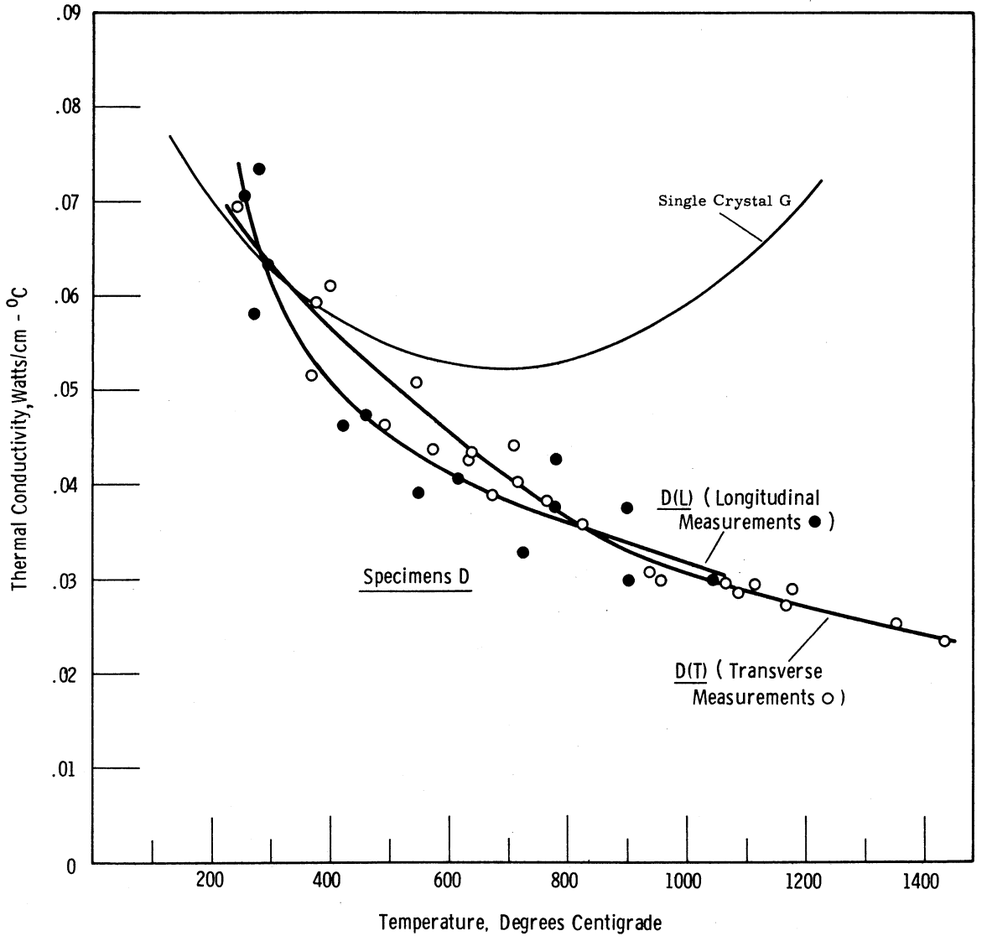

FIGURE 13

Thermal Conductivity of UO_2
(Hydrostatically Pressed and Sintered)

AEC-GE RICHLAND, WASH.

SPECIMENS 65, 68, 70 - CYLINDERS

Nonirradiated UO_2

Extruded, hydrostatically pressed, sintered

Specimen	65	68	70
Length	7.704 cm	7.622 cm	7.658 cm
Diameter	0.6325 cm	0.6350 cm	0.6375 cm
Weight	23.1457 g	24.2834 g	25.4589 g
Density	9.55 g/cc (87.1% TD)	10.06 g/cc (91.7% TD)	10.45 g/cc (95.3% TD)

Measured Data

Temp. °C	Thermal Cond. w/(cm)(°C)	Temp. °C	Thermal Cond. w/(cm)(°C)	Temp. °C	Thermal Cond. w/(cm)(°C)
90	0.0767	91	0.0752	105	0.0779
167	0.0679	167	0.0685	158	0.0718
221	0.0622	255	0.0597	190	0.0640
258	0.0618	313	0.0517	331	0.0538
299	0.0527	383	0.0470	388	0.0474
358	0.0505	478	0.0395	474	0.0397
438	0.0455	548	0.0374	608	0.0376
498	0.0390	609	0.0366	758	0.0302
555	0.0357				
641	0.0368				
734	0.0312				

SPECIMEN 1000 - CYLINDER

Nonirradiated UO_2

Machined from large hydrostatically pressed and sintered rod

Length	7.925 cm
Diameter	0.6299 cm
Weight	25.2492 g
Density	10.22 g/cc (93.2% TD)

Measured Data

Temperature °C	Thermal Conductivity watts/(cm)(°C)
88	0.0906
129	0.0811
187	0.0686
282	0.0601
362	0.0553
418	0.0508
526	0.0479

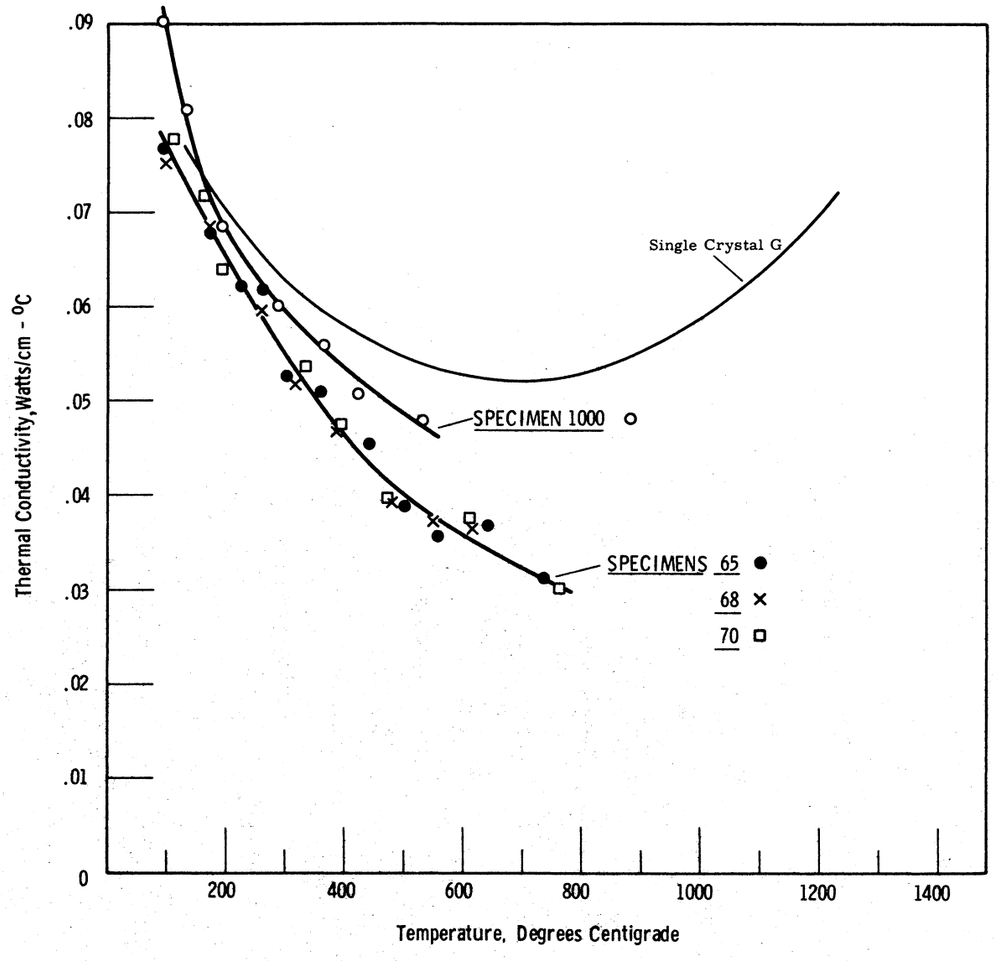

FIGURE 14

Thermal Conductivity of UO_2
(Extruded, Pressed and Sintered Cylinders)

SPECIMEN G - RECTANGULAR ROD

Nonirradiated UO_2 Crystal

Machined from arc-fused single crystal boule.

Length 4.464 cm
Rectangular cross-section 1.137 x 0.793 cm
Weight 43.8428 g
Density 10.89 g/cc (99.4% TD)

Measured Data

Series 1

Temperature °C	Thermal Conductivity watts/(cm)(°C)
143	0.0739
169	0.0714
170	0.0766
188	0.0724
203	0.0655
228	0.0672
290	0.0648
333	0.0630
360	0.0581
420	0.0550
421	0.0580
540	0.0517
561	0.0560
564	0.0579
644	0.0548
651	0.0527
707	0.0514
730	0.0505
839	0.0520
845	0.0529

Series 2

387	0.061
456	0.058
746	0.054
794	0.056
909	0.054
963	0.056
1011	0.067
1216	0.067

SPECIMEN 11 - CYLINDER

Irradiated UO_2 - 1.40×10^{18} f/cc

(Maximum UO_2 temperature during irradiation, <100 C)

Extruded, hydrostatically pressed, sintered.

Length 7.669 cm
Diameter 0.6375 cm
Weight 24.6495 g
Density 10.07 g/cc (91.8% TD)

Measured Data

Temperature °C	Thermal Conductivity watts/(cm)(°C)
57	0.0452
85	0.0415
140	0.0389
144	0.0428
175	0.0377
341	0.0398
384	0.0383
544	0.0345
613	0.0341
354	0.0416
225	0.0493

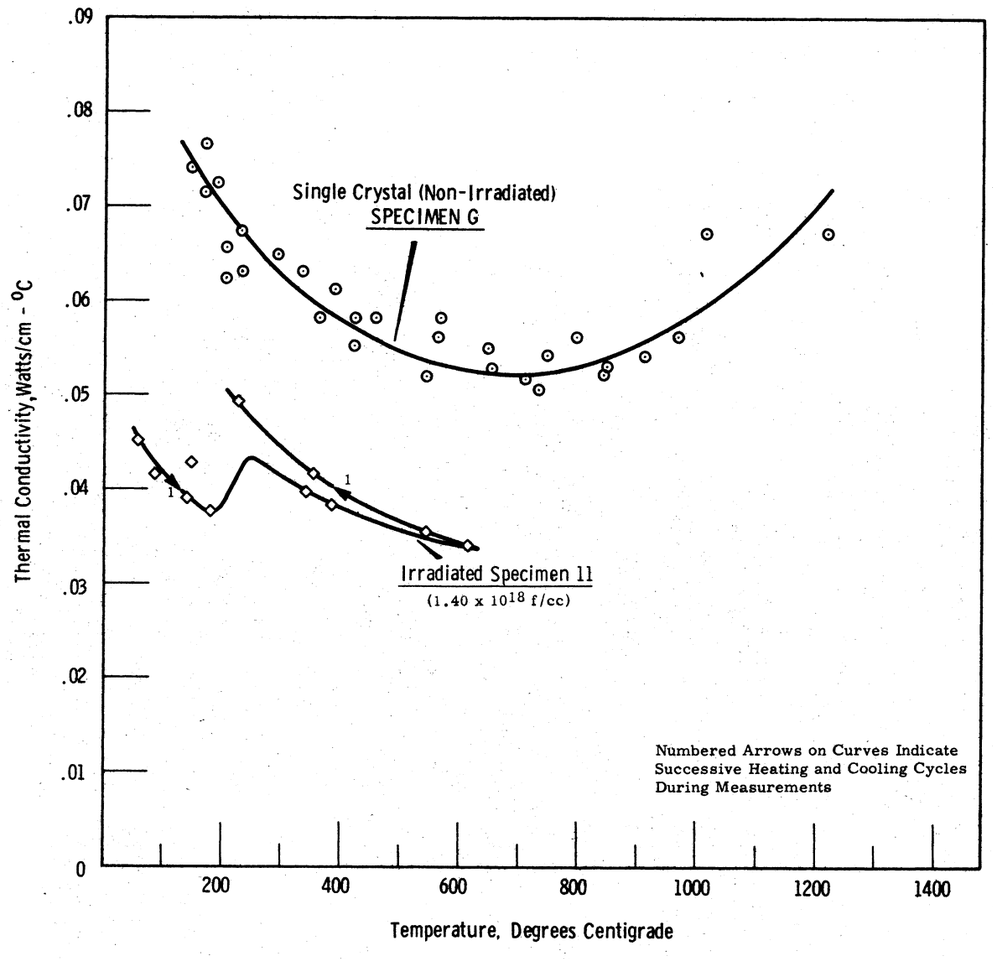

FIGURE 15

Thermal Conductivity of UO_2
(Single Crystal; Irradiated Sintered Cylinder 11)
(Maximum UO_2 temperature during irradiation, <100 C

AEC-GE RICHLAND, WASH.

SPECIMEN 19 - CYLINDER

Irradiated UO_2 - 4.11×10^{18} f/cc

(Maximum UO_2 temperature during irradiation, <100 C)

Extruded, hydrostatically pressed, sintered.

Length	7.675 cm
Diameter	0.6350 cm
Weight	25.0763 g
Density	10.32 g/cc (94.1% TD)

Measured Data*

Series 1

Temperature °C	Thermal Conductivity watts/(cm)(° C)
68	0.0407
121	0.0352
163	0.0301
199	0.0356

Series 2

Temperature °C	Thermal Conductivity watts/(cm)(°C)
84	0.0430
177	0.0378
329	0.0342
479	0.0346
265	0.0404
95	0.0442

* Values shown are based on upper and lower thermocouples only, to eliminate effect of faulty center thermocouple operating during this series of measurements.

AEC-GE RICHLAND, WASH.

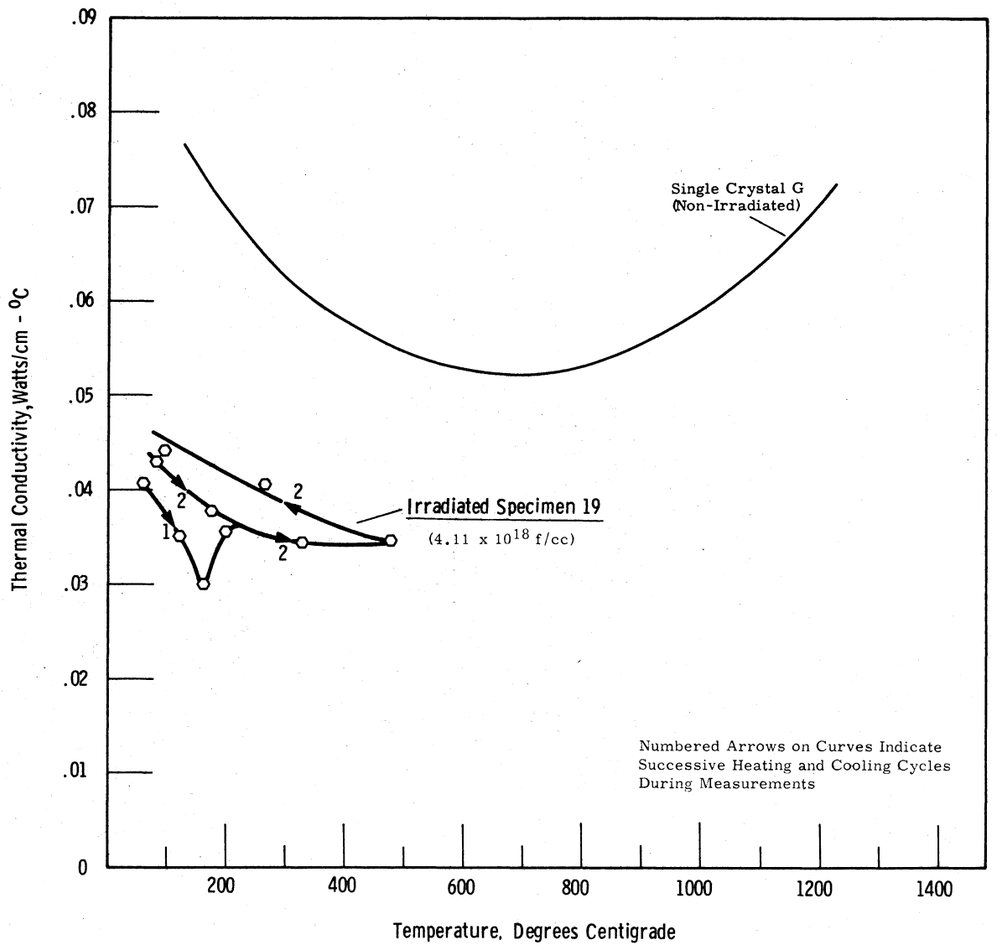

FIGURE 16

Thermal Conductivity of UO_2
(Irradiated Sintered Cylinder 19)
(Maximum UO_2 temperature during irradiation, <100 C

SPECIMEN 51 - CYLINDER

Irradiated UO_2 - 1.1×10^{19} f/cc

(Maximum UO_2 temperature during irradiation, <100 C)
Extruded, hydrostatically pressed, sintered.

Length	7.6634 cm
Diameter	0.6325 cm
Weight	24.9878 g
Density	10.37 g/cc (94.5% TD)

Measured Data

Series 1

Temperature °C	Thermal Conductivity watts/(cm)(°C)
59	0.0345
71	0.0339
86	0.0336
104	0.0327
144	0.0275
167	0.0306
267	0.0327
292	0.0317

Series 2

Temperature °C	Thermal Conductivity watts/(cm)(°C)
46	0.0519
58	0.0509
154	0.0397
157	0.0393
248	0.0325
268	0.0346
378	0.0318
400	0.0342
463	0.0363
482	0.0388
503	0.0342
504	0.0370
533	0.0371
533	0.0348
572	0.0358
606	0.0349
247	0.0454
231	0.0487

Series 3

Temperature °C	Thermal Conductivity watts/(cm)(°C)
61	0.0659
65	0.0576
76	0.0639
80	0.0607
736	0.0291
775	0.0270
803	0.0271
836	0.0279
886	0.0262

AEC-GE RICHLAND, WASH.

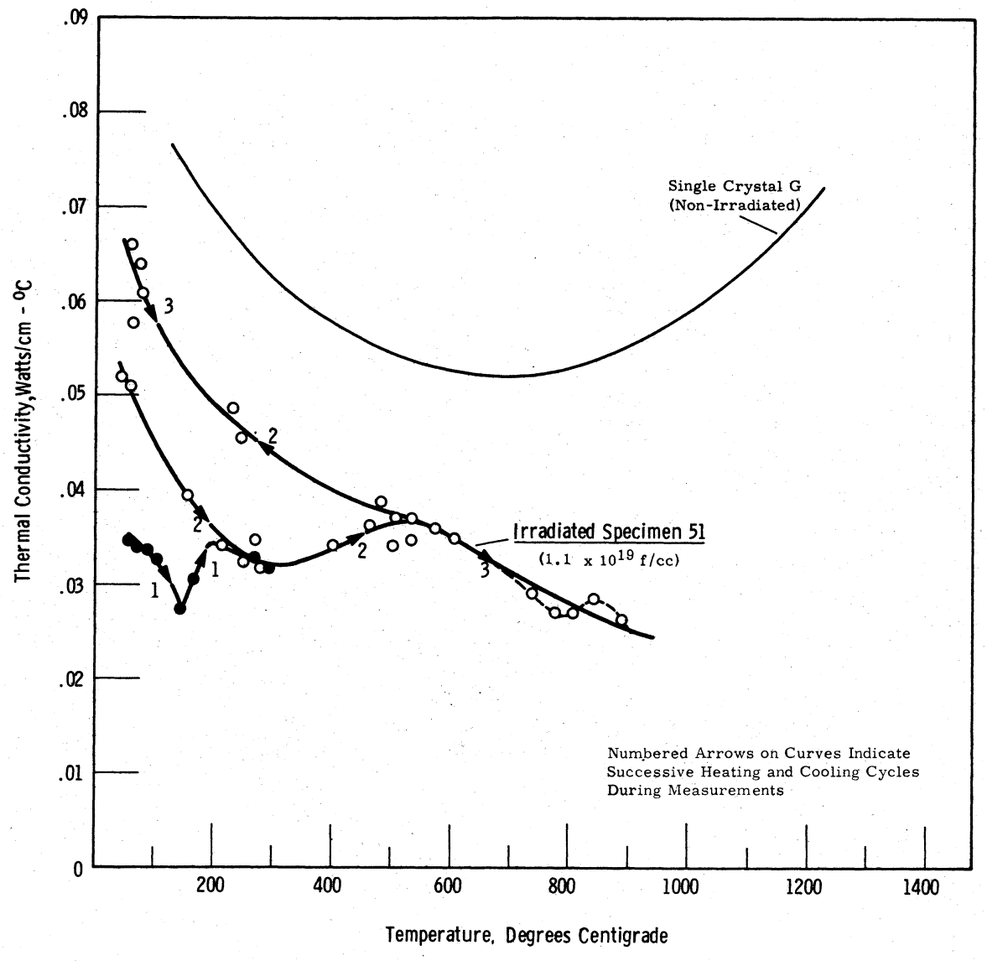

FIGURE 17

Thermal Conductivity of UO_2
(Irradiated Sintered Cylinder 51)
(Maximum UO_2 temperature during irradiation, <100 C)

REFERENCES

1. Belle, J. (ed.) "Uranium Dioxide", Properties and Nuclear Applications, pp. 177-189. Naval Reactors, Division of Reactor Development, USAEC. July, 1961.
2. Ross, A. M. Dependence of the Thermal Conductivity of Uranium Dioxide on Density, Microstructure, Stoichiometry and Thermal-Neutron Irradiation, CRFD-817. September, 1960.
3. Charvat, F. R. and W. D. Kingery. "Thermal Conductivity: XIII, Effect of Microstructure on Conductivity of Single-Phase Ceramics", J. Am. Ceram. Soc. 40: 306-15. 1957.
4. Kingery, W. D. "Thermal Conductivity: XIV, Conductivity of Multi-component Systems", J. Am. Ceram. Soc. 42: 617-27. 1959.
5. Shapiro, H. and R. M. Powers. High Conductivity UO_2. Terminal Report, SCNC-294. October, 1959.
6. Powers, R. M. "UO_2 Additives", Nucleonics 18, (10) p. 6. October, 1960.
7. Cohen, I., B. Lustman and J. D. Eichenberg. "Measurements of the Thermal Conductivity of Metal-Clad Uranium Oxide Rods During Irradiation", J. Nuc. Materials 3: 331-353. 1961.
8. Daniel, J. L. Personal Data.
9. deHalas, D. R. and G. R. Horn. Evolution of Uranium Dioxide Structure During Irradiation of Fuel Rods, (J. Nuc. Materials) HW-SA-2650. June, 1962.
10. Loeb, A. L. "Thermal Conductivity: VIII, A Theory of Thermal Conductivity of Porous Materials", J. Am. Ceram. Soc. 37: 96-99. 1954.
11. Boegli, J. and R. Deissler. Measured Effective Thermal Conductivity of UO_2 Powder in Various Gases and Gas Mixtures, NACA-RM-E-54L10. 1955.
12. Snyder, T. and R. Kamm. Some Physical Constants Important in the Design of an Atomic Power Plant, C-192. (Declassified December 12, 1955).
13. Anthony, A. J., C. E. Burdg and R. J. Sanderson. "Out-of-Pile Thermal Testing of UO_2 Fuel Elements", Transactions of the American Nuclear Society, 1962 Annual Meeting, Boston, Massachusetts, June 18-21, 1962. pp. 236-7.
14. Murtha, B. E. and W. P. Chernock. The Development and Testing of the UO_2 Fuel Element System (Summary Report), CEND-141. June, 1961.
15. D'hont, M., E. V. Bemden and J. Van der Speck. "Description of the Belgonucleaire - C.E.N. Plutonium Project", Topical Report, BN-6209-13, Euratom/United States (Proceedings, ANS Topical Meeting, Richland, Washington, September 13-14, 1962.)

16. Kingery, W. D., et al. "Thermal Conductivity: X, Data for Several Pure Oxide Materials Corrected to Zero Porosity", J. Am. Ceram. Soc. 37: 107-10. 1954.

17. Bates, J. L. "Thermal Conductivity of UO_2 Improves at High Temperatures", Nucleonics 19 (6) 83-87. June, 1961.

18. Reiswig, R. D. "Thermal Conductivity of UO_2 to 2100 C", J. Am. Ceram. Soc. 44: 48-49. 1961.

19. Howard, V. C. and T. F. Gulvin. Thermal Conductivity Determinations on Uranium Dioxide by a Radial Flow Method, IGR-51 (R D/C). 1961.

20. Bates, J. L. Personal Communication.

21. Burke, J. E. (ed.) Progress in Ceramic Science, Vol. 2: 182-235. Pergamon Press, New York. 1962.

22. Bloch, J. "Restauration Thermique du Parametre de L'UO_2 Faiblement Irradie", J. Nuc. Materials 3: 237-8. 1961.

23. Ross, A. M. A Literature Survey on the Measurement of Thermal Conductivity of Several Solids Including Uranium Dioxide, CRFD-762. March, 1958.

24. Johnson, W. T. K. The Thermal Conductivity of Solids at High Temperatures - A Bibliography, PB 161118. (Office of Technical Services, U. S. Dept. of Commerce.) June, 1959.

25. Parker, W. J., et al. A Flash Method of Determining Thermal Diffusivity, Heat Capacity and Thermal Conductivity, USNRDL-TR-424. 1960.

26. Van Dusen, M. S. and S. M. Shelton. "Apparatus for Measuring Thermal Conductivity of Metals up to 600 C", J. Research National Bureau Standards, 12: 429-440. 1934.

INTERNAL DISTRIBUTION

Copy Number	
1	F. W. Albaugh
2	H. J. Anderson
3	R. J. Anicetti
4	W. J. Bailey
5	J. L. Bates
6	D. W. Brite
7	J. B. Burnham
8	S. H. Bush
9	J. J. Cadwell
10	D. F. Carroll
11	J. A. Christensen
12 - 31	J. L. Daniel
32	D. R. deHalas
33	K. Drumheller
34	E. A. Evans
35	M. D. Freshley
36	J. J. Hauth - G. R. Horn
37	Y. B. Katayama
38	J. O. McPartland - M. K. Millhollen
39	L. E. Mills - J. E. Minor - L. P. Murphy
40	W. E. Roake
41	R. E. Skavdahl
42	R. C. Smith
43	I. D. Thomas
44	M. T. Walling
45	O. J. Wick
46	R. D. Widrig
47	W. H. Woodcock
48	300 Files
49	Record Center
50	Technical Publications
51 - 70	Extra

EXTERNAL DISTRIBUTION (SPECIAL)

Number of Copies	
20	Instrumentation Division Battelle Memorial Institute Columbus, Ohio Attn: J. Matolich, Jr. (10) H. W. Deem (10)
2	G. E. Technical Data Center, Schenectady
1	HOO - Technical Information Library

EXTERNAL DISTRIBUTION

Number of Copies	
3	Aberdeen Proving Ground
1	Aerojet-General Corporation
1	Aerojet-General Nucleonics
8	Aeronautical Systems Division
1	Aeroprojects Incorporated
1	Allis-Chalmers Manufacturing Company
1	Allis-Chalmers Manufacturing Company, Schenectady
1	Allis-Chalmers Manufacturing Company, Washington
1	Allison Division–GMC
10	Argonne National Laboratory
1	Armour Research Foundation
1	Army Missile Command
1	AEC Scientific Representative, Belgium
1	AEC Scientific Representative, France
1	AEC Scientific Representative, Japan
3	Atomic Energy Commission, Washington
4	Atomic Energy of Canada Limited
4	Atomics International
4	Babcock and Wilcox Company
2	Battelle Memorial Institute
2	Beers (Roland F.), Inc.
1	Beryllium Corporation
1	Bridgeport Brass Company
1	Bridgeport Brass Company, Ashtabula
2	Brookhaven National Laboratory
1	Bureau of Mines, Albany
1	Bureau of Ships (Code 1500)
1	Carborundum Company
1	Chance Vought Corporation
1	Chicago Patent Group
1	Clevite Corporation
1	Combustion Engineering, Inc.
1	Combustion Engineering, Inc. (NRD)
1	Defence Research Member
1	Denver Research Institute
1	Department of the Army
1	Dow Chemical Company (Rocky Flats)
4	duPont Company, Aiken
1	duPont Company, Wilmington
1	Federal Aviation Agency
1	Frankford Arsenal
1	Franklin Institute of Pennsylvania
1	Fundamental Methods Association
2	General Atomic Division
1	General Dynamics/Astronautics (NASA)
1	General Dynamics/Convair, San Diego (BUWEPS)
2	General Dynamics/Fort Worth
2	General Electric Company, Cincinnati

EXTERNAL DISTRIBUTION (Contd)

Number of Copies	
1	General Electric Company, San Jose
1	General Electric Company, St. Petersburg
1	General Nuclear Engineering Corporation
1	General Scientific Corporation
1	General Telephone and Electronic Laboratories, Inc.
1	Goodyear Atomic Corporation
2	Iowa State University
2	Jet Propulsion Laboratory
3	Knolls Atomic Power Laboratory
1	Lockheed Georgia Company
1	Lockheed Missiles and Space Company (NASA)
3	Los Alamos Scientific Laboratory
1	M & C Nuclear, Inc.
1	Mallinckrodt Chemical Works
1	Maritime Administration
1	Martin-Marietta Corporation
1	Materials Research Corporation
1	Mound Laboratory
1	NASA Lewis Research Center
2	NASA Scientific and Technical Information Facility
2	National Bureau of Standards
1	National Bureau of Standards (Library)
2	National Lead Company of Ohio
1	Naval Postgraduate School
3	Naval Research Laboratory
1	New Brunswick Area Office
1	Nuclear Materials and Equipment Corporation
1	Nuclear Metals, Inc.
1	Office of Assistant General Counsel for Patents (AEC)
2	Office of Naval Research
1	Office of Naval Research (Code 422)
1	Ordnance Materials Research Office
1	Ordnance Tank-Automotive Command
4	Phillips Petroleum Company (NRTS)
1	Picatinny Arsenal
1	Power Reactor Development Company
3	Pratt and Whitney Aircraft Division
1	Purdue University
1	RAND Corporation
1	Rensselaer Polytechnic Institute
1	Research Analysis Corporation
2	Sandia Corporation, Albuquerque
1	Sandia Corporation, Livermore
1	Space Technology Laboratories, Inc.
1	Sylvania Electric Products, Inc.
1	Technical Research Group
1	Tennessee Valley Authority

EXTERNAL DISTRIBUTION (Contd)

Number of Copies	
2	Union Carbide Nuclear Company (ORGDP)
5	Union Carbide Nuclear Company (ORNL)
1	Union Carbide Nuclear Company (Paducah Plant)
1	United Nuclear Corporation (NDA)
1	United Nuclear Corporation (OMC)
1	U. S. Geological Survey, Denver
1	U. S. Geological Survey, Menlo Park
1	U. S. Geological Survey, Washington
1	U. S. Patent Office
2	University of California, Berkeley
2	University of California, Livermore
1	University of Puerto Rico
1	Watertown Arsenal
1	Western Reserve University (Major)
4	Westinghouse Bettis Atomic Power Laboratory
1	Westinghouse Electric Corporation
1	Westinghouse Electric Corporation (NASA)
1	Yankee Atomic Electric Company
325	Division of Technical Information Extension
75	Office of Technical Services, Washington